PAPER

Check for updates

Mitigation of apricot quality loss and waste during high-temperature processing *via* sonication and electric field pretreatments

Nida Kanwal,[ab] Min Zhang, [ID] *[ac] Erum Bux[d] and Wang Xiaojing[e]

This study systematically evaluated the sequential application of 2% $CaCl_2$ soaking, sonication (150–300 W, 2–5 min), and pulsed electric field (PEF; 1.5–3.0 kV cm^{-1}, 30–90 min) pretreatments on firmness retention, weight loss, and bioactive compounds in apricot pieces prior to blanching at 85 °C for 3 min, employing a response surface methodology (RSM) design encompassing 27 treatments (T1–T27) alongside controls (C1: blanching only; C2: $CaCl_2$ + sonication; C3: $CaCl_2$ + PEF). Conventional blanching (C1) reduced firmness to 0.23 N (baseline) and incurred 20% weight loss, while the optimized treatment T10 (200 W/ 3 min sonication + 1.5 kV cm^{-1} 30 min PEF) enhanced post-blanching firmness to 0.3335 N, achieving 45% retention ($p < 0.05$ *vs.* C1; superior to C2: 20%, C3: 27%), and curtailed weight loss to 9% (55% reduction). Firmness peaked at moderate sonication/PEF intensities but declined under extreme conditions due to over-permeabilization, with RSM plots revealing significant quadratic interactions ($r = 0.92$; firmness-weight loss). Bioactive retention in T10 surpassed C1, yielding a total polyphenol content (TPC) of 14.9 ± 0.8 mg GAE per g DW (19% higher), a total flavonoid content (TFC) of 6.6 ± 0.4 mg CE per g DW (25% higher), DPPH scavenging of 54 ± 4.0% (20% higher), and a total anthocyanin content (TAC) of 3.4 ± 0.2 mg C3G per g DW (36% higher; ANOVA, Tukey's HSD, $p < 0.05$), outperforming single pretreatments and correlating strongly with firmness ($r = 0.88$; TPC-firmness). Fourier-transform infrared spectroscopy (FTIR) confirmed intensified pectin cross-linking (1730 and 1620 cm^{-1}) and preserved glycosidic bonds in T10. The enhanced textural stability in T10 was further attributed to PME mediated demethylation of pectin, facilitating Ca^{2+}–pectin cross-linking and strengthening the middle lamella structure, while X-ray diffraction (XRD) indicated elevated relative crystallinity (28.2% *vs.* 19.1% in C1), underpinning synergistic Ca^{2+}-mediated pectin stabilization, cavitation enhanced impregnation, and electroporation driven uniformity against thermal degradation. These findings demonstrate combined pretreatments as a viable strategy to mitigate blanching-induced quality loss in apricot pieces, enhancing process yield, texture, and nutritional value for sustainable stone fruit processing.

Sustainability spotlight

This research addresses the critical challenge of post-harvest food loss by introducing innovative, non-thermal pretreatments—sonication and pulsed electric field—to significantly reduce quality degradation and waste in apricots during high-temperature processing. By enhancing processing efficiency and extending shelf-life, this approach directly conserves resources, reduces energy consumption, and minimizes waste, contributing to a more resilient and sustainable food system.

[a]State Key Laboratory of Food Science and Resources, Jiangnan University, 214122 Wuxi, Jiangsu, China. E-mail: min@jiangnan.edu.cn; Fax: 0086-(0)510-85807976; Tel: +86-510-85877225

[b]Jiangsu Province International Joint Laboratory on Fresh Food Smart Processing and Quality Monitoring, Jiangnan University, 214122 Wuxi, Jiangsu, China

[c]China General Chamber of Commerce Key Laboratory on Fresh Food Processing & Preservation, Jiangnan University, 214122 Wuxi, Jiangsu, China

[d]School of Biotechnology, Jiangnan University, Wuxi, China

[e]Haitong Food Group Company, Cixi, Zhejiang, China

1. Introduction

High temperature processing such as blanching is indispensable in apricot preservation chains but simultaneously drives substantial quality loss and economic [1]waste. Blanching inactivates enzymes and reduces microbial load, yet the associated thermal load accelerates softening, tissue disintegration, drip loss, and degradation of color and bioactive compounds, ultimately diminishing product yield and nutritional and sensory value.[1] In the apricot industry, this over softening translates directly into flesh loss during subsequent handling and cutting,

with weight losses on the order of 20% representing a major bottleneck for process efficiency and sustainability.[2] At the same time, consumers increasingly demand minimally processed apricot products with fresh like texture and high retention of polyphenols, flavonoids, and anthocyanins, as well as antioxidant activity, creating a pressing need for technologies that decouple enzyme inactivation from severe structural and nutritional damage.[3,4]

Apricot (*Prunus armeniaca L.*) is particularly sensitive to thermal treatments due to its delicate parenchyma tissue and high content of thermolabile bioactive compounds such as carotenoids, phenolics, and vitamin C.[5] Conventional hot water or hot air blanching can cause rapid cell wall breakdown, pectin depolymerization, and loss of middle lamella integrity,[6] resulting in a marked decrease in firmness and pronounced shrinkage and drip loss. In apricot pieces and other stone fruits, increasing processing temperature and time has been associated with color deterioration, shrinkage, and progressive degradation of phenolic compounds and ascorbic acid, even when enzymatic inactivation is achieved.[7] These structural and compositional changes not only compromise texture and appearance but also reduce functional value, limiting the potential of apricot based products in health oriented markets.[8] Despite numerous process innovations, high temperature blanching remains one of the least optimized steps regarding the simultaneous control of firmness, flesh yield, and nutrient retention. To mitigate heat induced quality damage, recent research has explored a range of physical pretreatments such as sonication, pulsed electric fields (PEFs),[9] and advanced blanching methods as tools to tailor tissue microstructure prior to high temperature exposure. Sonication can generate cavitation, micro-streaming, and mechanical stresses that modify cell walls and membranes, promote mass transfer, and, when properly controlled, enhance drying and improve rehydration while preserving color and bioactive compounds in various fruits.[10] For example, sonication-assisted osmotic dehydration has been shown to enhance antioxidant retention, maintain brighter color, and reduce shrinkage in litchi, plums, and other fruits, reflecting a more open and yet structurally resilient microstructure. However, excessive sonication intensity or exposure can lead to cell rupture and undesirable softening, and most studies have focused on drying rather than on optimizing firmness retention across a subsequent blanching step.[11]

PEF has emerged as another promising non-thermal or mild-thermal technology that uses short, high voltage pulses to induce electroporation of plant cell membranes.[11] In fruits such as tomatoes, kiwifruit,[12] and mango, PEF pretreatment has improved peeling efficiency and reduced peeling losses while maintaining or even enhancing textural and nutritional quality relative to conventional blanching or chemical peeling.[13] PEF has also been widely reported to increase the apparent extractability and measured content of phenolic compounds and anthocyanins, largely by facilitating diffusion from disrupted cell compartments into surrounding matrices. Nonetheless, most PEF studies have targeted processing endpoints such as peeling,[13] juice or polyphenol extraction, or drying kinetics, rather than the controlled preservation of fruit flesh integrity and firmness during high-temperature blanching of fresh like pieces.[12]

In parallel, calcium salt pretreatments especially $CaCl_2$ solutions have long been exploited to strengthen plant tissue by promoting pectin cross-linking within the cell wall matrix.[14] Calcium ions can interact with free carboxyl groups of homogalacturonan chains to form "egg-box" structures, thereby increasing pectin rigidity, reducing solubilization during heating, and improving firmness retention in blanched fruits and vegetables. Endogenous pectin methylesterase (PME) contributes to this reinforcement by catalyzing the demethylesterification of homogalacturonan domains,[15] increasing the density of Ca^{2+}-accessible carboxyl groups and thereby promoting more extensive pectate network cross-linking during thermal processing. Yet, calcium treatments alone often fail to fully counteract the disruptive effects of prolonged heating and associated acid or enzyme catalyzed pectin depolymerization, particularly in soft fruits such as apricot.[16] Moreover, the interaction between Ca-mediated tissue stabilization and emerging physical pretreatments such as sonication and PEF has not been systematically characterized for stone fruits undergoing industrially relevant blanching conditions. Taken together, the literature highlights three critical gaps that constrain the development of robust, high quality apricot processing chains. First, while numerous studies have evaluated the impact of drying methods, storage conditions, or single pretreatments on apricot quality, there is a lack of integrative work that explicitly targets blanching-induced over softening and associated flesh loss in fresh like apricot pieces. Second, most investigations examine sonication, PEF, or $CaCl_2$ pretreatments in isolation, making it difficult to understand potential synergistic or antagonistic effects when these technologies are combined and sequentially applied prior to high-temperature processing. Third, despite frequent reporting of color and global antioxidant metrics, limited attention has been paid to quantitative relationships between pretreatment conditions, firmness retention and flesh yield, and specific nutritional markers such as total polyphenols, flavonoids, and anthocyanins after blanching. As a result, processing decisions are often guided by qualitative observations rather than by optimized, mechanistically informed treatment combinations that jointly minimize waste and preserve nutritional and textural quality.

Although the above technologies have each shown promise in other fruits, their combined and mechanistically guided application to apricot remains largely unexplored. Unlike many fruits, apricot tissue exhibits high pectin solubility and rapid thermo-softening even under mild heat, making it an excellent model to study the interplay between calcium mediated reinforcement and physical membrane disruption under combined pretreatments.[15,17] Exploring the synergistic effects of sonication, PEF, and $CaCl_2$ in this context not only addresses an industrially relevant challenge, flesh loss during blanching, but also advances a mechanistic understanding that has not been established in previous fruit systems. The present study addresses these gaps by systematically investigating the mitigation of apricot quality loss and waste during high temperature blanching through the combined application of $CaCl_2$ soaking, sonication, and pulsed electric field pretreatments. Firm ripe apricots were selected and standardized by size, soluble solids, and maturity stage to minimize biological

variability and enable robust comparisons among treatments. The process sequence, CaCl$_2$ soaking, sonication in CaCl$_2$ solution, PEF application to apricot pieces, followed by blanching at 85 °C for 3 min, was designed to emulate industrial blanching while allowing mechanistic interrogation of how each pretreatment step modulates tissue integrity and compound retention. By varying sonication power (150–300 W), sonication time (2–5 min), PEF intensity (1.5–3.0 kV cm^{-1}), and PEF duration (30–90 min) within a structured response surface methodology design, this work explores a broad processing space and identifies optimal combinations for concurrent physical and nutritional quality preservation.

This study innovates by explicitly quantifying firmness retention, flesh loss reduction, and detailed nutritional profiling relative to conventional blanching controls. The structured experimental design systematically evaluates pretreatment interactions across a broad processing space to identify optimal combinations that simultaneously enhance structural integrity and preserve bioactive compounds. Overall, this work contributes to the high impact literature on fruit processing by (i) focusing on a thermally sensitive stone fruit and a technologically relevant high-temperature blanching step; (ii) systematically combining CaCl$_2$ soaking, sonication, and PEF into an integrated pretreatment strategy; (iii) quantifying their effects on firmness retention, flesh loss, and key nutritional and antioxidant markers following blanching; and (iv) identifying optimal pretreatment combinations that minimize waste while enhancing nutritional quality relative to conventional blanching. By clarifying the interplay between treatment intensity, exposure time, tissue integrity, and bioactive retention, the study offers actionable guidance for designing low-waste,[18] high-quality apricot processing operations and provides a transferable framework for applying combined non-thermal pretreatments to other heat sensitive fruits in modern food supply chains.

2. Materials and methods

2.1 Sample preparation

Apricot (*Prunus armeniaca L.*) fruits,[19] Youyi cultivar, were procured from a local market in Wuxi, Jiangsu Province, China, affiliated with Jiangnan University. Mature fruits of uniform size (approximately 40–50 mm equatorial diameter) and consistent ripeness (firm ripe stage, total soluble solids 12–15° Brix) were selected to minimize variability in physicochemical

properties across replicates. Post-procurement, fruits were immediately transported to the laboratory in insulated containers at 4 ± 1 °C and stored at 2–4 °C with 85–90% relative humidity for up to 24 h prior to processing, ensuring minimal physiological changes and microbial growth while maintaining firmness and quality. Fruits were thoroughly rinsed under running potable water to remove surface contaminants, followed by surface sterilization with 0.1% (w/v) sodium hypochlorite for 1 min and two subsequent rinses with sterile distilled water. Pits were aseptically removed using a stainless steel knife. Fruit flesh was excised into pieces of 2 × 2 × 2 cm^3 (about 8 g per piece) with a Laboratory Manual Bench Cutting Knife (TOB New Energy, China) to ensure uniform geometry and reproducible surface area-to-volume ratio for treatment exposure. Prepared samples were randomly allocated into treatment groups (n = 12–15 per group), each corresponding to a predefined combination of sonication power (W), PEF strength (kV cm^{-1}), and exposure duration (min), with untreated controls included for baseline comparison.

2.2 Methodology: RSM design matrix

Apricot pieces were first soaked in 2% CaCl$_2$ solution (at room temperature) and then subjected to sonication in the same solution at specified power (150, 200, or 300 W) and duration (2, 3, or 5 min). Post-sonication, pieces were removed from the solution, cooled down, and subjected to PEF treatment (pieces only) at intensities of 1.5, 2.5, or 3.0 kV cm^{-1} for 30, 60, or 90 min. Finally, samples underwent blanching at 85 °C for 3 min. The control (C1) received only blanching without pretreatments; C2 and C3 tested individual sonication or PEF effects, respectively. Table 1 details the RSM[20] design encompassing 27 combinatorial treatments (T1–T27) across sonication (150–300 W, 2–5 min) and PEF (1.5–3.0 kV cm^{-1}, 30–90 min) parameters following 2% CaCl$_2$ soaking (25 ± 2 °C for 10 minutes), plus controls C1–C3.

2.3 Sonication pretreatment

Sonication was performed using a lab-scale ultrasonic water bath (SK3300H, KUDOS Analytical Instrument Co., Ltd, Jiangsu, China; 20 kHz frequency; nominal powers of 150 W, 200 W, or 300 W) equipped with automatic temperature control and an inbuilt digital thermometer. Apricot piece samples (about 100 g, 12–15 pieces per treatment) were processed *via* indirect contact

Table 1 RSM design matrix for combined CaCl$_2$–sonication–PEF pretreatments prior to apricot blanching (27 treatments + 3 controls)

Samples	CaCl$_2$ 2%	Sonication (W min^{-1})	PEF (kV cm^{-1} min^{-1})	Blanching
T1-T9	Yes	150/2	1.5/30, 2.5/30, and 3.0/30 1.5/60, 2.5/60, and 3.0/60 1.5/90, 2.5/90, and 3.0/90	85 °C/3 min
T10-T18	Yes	200/3	(Same 9 combinations as above)	85 °C/3 min
T19-T27	Yes	300/5	(Same 9 combinations as above)	85 °C/3 min
C1 (control)	No	None	None	85 °C/3 min
C2	Yes	200/3	None	85 °C/3 min
C3	Yes	None	1.5/30	85 °C/3 min

immersion in a covered water bath container. Treatments T1–T9 received 150 W for 2 min each, T10–T18 received 200 W for 3 min each, and T19–T27 received 300 W for 5 min each, with all 27 treatments processed separately. The system maintained 25 ± 2 °C throughout *via* integrated thermostat regulation. Post-sonication, samples were immediately cooled to 4 °C prior to subsequent PEF treatments.

2.4 Pulsed electric field (PEF) pretreatment

PEF pretreatment was carried out using a lab-scale PEF system comprising a high voltage pulse generator, capacitor bank, switching unit, and a customized treatment chamber designed for solid fruit pieces. Apricot pieces assigned to PEF treatments were positioned within the chamber in a non-immersed configuration, ensuring that samples were not in direct contact with the electrodes and were not suspended in a liquid medium, while maintaining a fixed parallel plate electrode gap of 5 cm to achieve the desired electric field strengths. The applied electric field intensity was set at 1.5, 2.5, or 3.0 kV cm^{-1}, delivered as monopolar pulses with a pulse width of 50 μs and a pulse repetition frequency of 10 Hz, and the total treatment times were 30, 60, or 90 min depending on the experimental combination, corresponding to a specific energy input of approximately 2.7 kJ kg^{-1}. These operating conditions fall within the range reported for moderate-intensity PEF treatments aimed at inducing reversible or limited irreversible electroporation in plant tissues while avoiding extensive structural destruction. The selection of field strength, pulse width, frequency, and treatment duration was guided by previous PEF studies on fruits and vegetables focused on texture preservation and mass transfer enhancement, complemented by preliminary trials on apricot that identified processing windows capable of enhancing firmness retention and reducing softening without causing visible burning, excessive tissue breakdown, or undesired heating. During treatment, voltage and current waveforms were periodically monitored using an oscilloscope and a current probe to verify pulse stability and to calculate specific energy input, and the chamber temperature was kept below the threshold for noticeable thermal effects by intermittent operation and external cooling as needed. Extended 30–90 min exposures used cumulative low energy pulses (2.7 kJ kg^{-1} total) for solid piece diffusion (*vs.* ms for liquids), with monitored waveforms confirming no electrolysis (no Cl$_2$ evolution), temperature rise less than 50 °C *via* cooling and energy 10× lower than high intensity PEF. Immediately after completion of PEF exposure under each condition, apricot samples were removed from the chamber and subjected to high temperature blanching.

2.5 Blanching

Blanching was performed using a controlled-temperature water bath system (KUDOS Analytical Instrument Co., Ltd, Jiangsu, China) equipped with an integrated thermostat, digital thermometer, and insulated cover to maintain precise heating and minimize evaporative losses. Pretreated apricot pieces (approximately 100 g per batch, 12–15 pieces) were gently

immersed in 300 mL of deionized water (electrical conductivity <1 μS cm^{-1}) within heat-resistant borosilicate glass beakers (ratio of sample mass to water volume: 1 : 3), ensuring complete submersion without overcrowding to facilitate uniform heat penetration. The beakers were then placed in the preheated water bath, and the system temperature was rapidly stabilized at 85 ± 1 °C under continuous stirring and monitoring, with blanching conducted for exactly 3 min from the moment the sample core temperature reached 85 °C (verified by inserting a fine tip thermocouple into representative pieces). This time–temperature combination was selected based on preliminary optimization trials and literature precedents for achieving peroxidase inactivation in stone fruits while limiting excessive softening and nutrient leaching. Upon completion, beakers were immediately transferred to an ice water bath (0–2 °C) for rapid cooling to below 10 °C within 1 min, followed by gentle draining on sterile mesh screens to remove surface moisture without mechanical agitation. Treated samples were then patted dry with lint-free paper, weighed for yield calculations, and allocated for subsequent physicochemical analyses, with all operations replicated (*n* = 12–15 per treatment group) under aseptic conditions to prevent microbial contamination.

2.6 Firmness measurement

Firmness of blanched apricot pieces was determined using a TA.XTC texture analyzer (BosinTech, China) equipped with a 50 N load cell, following the standardized compression protocol described by Gull *et al.*, 2021. Individual pieces were centrally positioned on a heavy duty test platform with the flattest face downward, and a cylindrical TA/2 probe (5 mm diameter) was applied perpendicularly to compress the sample to 30% strain. Instrument parameters were set as follows: a trigger force of 3.0 g, a pre-test speed of 2.0 mm s^{-1}, a test speed of 1.0 mm s^{-1}, a post-test speed of 2.0 mm s^{-1}, and a 10 s data acquisition interval to capture peak force stability. Maximum compression force (*N*) was recorded as the firmness index,[21] with measurements performed in triplicate per sample (*n* = 12–15 per treatment group) at ambient temperature (20 ± 2 °C) and a relative humidity of 50–60%, ensuring minimal dehydration between replicates. Firmness retention (%) was calculated relative to the untreated blanched control (C1).

2.7 Weight loss measurement

Weight loss due to blanching-induced moisture evaporation and tissue softening was quantified gravimetrically for each apricot sample using an analytical balance (precision ± 0.001 g; Mettler Toledo, China) with reference to the protocol outlined by Abidi *et al.* (2023).[22] Uniform batches of pre-treated apricot pieces were weighed immediately prior to immersion in the blanching setup, subjected to the full pretreatment sequence (CaCl$_2$ soaking, sonication, and PEF) followed by hot water blanching at 85 °C for 3 min, and then rapidly cooled in an ice bath (0–2 °C) for 1 min, surface-drained on sterile mesh sieves for 30 s, and gently patted dry with lint-free absorbent paper to remove excess moisture without compressing the tissue. Final mass (MfM_fMf) was recorded within 2 min post-cooling to

minimize post-blanching evaporation artifacts. Absolute weight loss (WL, g) was calculated as $W_L = M_0 - M_f$ $W_L = M\_0 - M\_f$ $W_L = M_0 - M_f$, and percentage weight loss (WL%) was determined using eqn (1):

$$W_L = ((M_0 - M_f)/M_0) \times 100 \tag{1}$$

where M_0 M_0 M_0 is the initial mass before blanching and M_f M_f M_f is the final mass after blanching and cooling. Measurements were conducted in triplicate per treatment group, with samples handled under controlled humidity conditions (50–60% RH) at 20 ± 2 °C to ensure reproducibility, enabling direct assessment of pretreatment efficacy in mitigating blanching-associated food waste (FW).

2.8 Extraction of polyphenolic compounds

A 1 g sample of apricot tissue was placed into a 100 mL amber glass bottle. To this, 50 mL of an 80% methanol solution, containing 0.1% hydrochloric acid, was added. The mixture was stirred for 1 hour using a magnetic stirrer to ensure thorough mixing. Afterward, the mixture was centrifuged at 4400 rpm for 10 minutes. This extraction process was repeated three times, and the resulting supernatants were combined. The pooled extract was concentrated to a final volume of 1 mL, transferred to a graduated amber bottle, and diluted with 80% methanol to a total volume of 15 mL to prepare the test solution.

2.9 Determination of total polyphenol content (TPC)

TPC was quantified using the Folin-Ciocalteu colorimetric method as outlined in previous studies by Raposo et al., 2024 with slight modifications.[23,24] For this assay, 25 μL of the sample (both test and gallic acid standard solutions) were pipetted into a 96-well microplate. Next, 125 μL of 0.2 N Folin–Ciocalteu reagent was added to each well, followed by shaking and allowing the reaction to proceed at room temperature for 6 minutes. Subsequently, 100 μL of 0.075 g mL^{-1} sodium carbonate solution was added, mixed thoroughly, and incubated in the dark for 60 minutes. The absorbance was measured at 765 nm. Gallic acid standard solutions of 0.01, 0.03, 0.06, 0.12, 0.2, 0.4, and 0.5 mg mL^{-1} were used to create a calibration curve. In cases where the test sample concentration exceeded the standard range, the sample was appropriately diluted before measurement. The TPC was expressed as milligrams of gallic acid equivalents (GAE) per gram of dry weight (DW). All assays were conducted in triplicate for each treatment to ensure consistency and accuracy of the results.

$$TPC(\text{mg GAE per g DW}) = \left(\frac{A_{sample} - A_{blank}}{A_{standard}} \right) \times C_{standard}$$
$$\times \frac{V_{total}}{V_{sample}} \times \frac{1}{m_{sample}}$$

where A_{sample} = absorbance of the sample, A_{blank} = absorbance of the blank, $A_{standard}$ = absorbance of the standard, $C_{standard}$ = concentration of the standard, V_{total} = total volume of the extract, V_{sample} = volume of the sample used, and m_{sample} = mass of the sample.

2.10 Determination of total flavonoid content (TFC)

The TFC content was measured using the sodium nitrite–aluminum chloride method, as described by Chen et al., 2021 with slight modifications.[25] To begin, 200 μL of the sample (both test and catechin standard solutions) was transferred into a 1.5 mL centrifuge tube. Then, 550 μL of a 5% sodium nitrite solution was added to the tube, and the mixture was vortexed and allowed to react for 5 minutes. After the reaction, 75 μL of a 10% aluminum chloride solution was added, and the mixture was vortexed again, allowing the reaction to continue for an additional 6 minutes. Finally, 500 μL of 1 mol L^{-1} sodium hydroxide solution was introduced, and the mixture was vortexed once more. The absorbance of the resulting solution was measured at 510 nm using a UV-vis spectrophotometer. Catechin was used as the reference standard, and a calibration curve was prepared using catechin standards ranging from 0 to 100 μg mL^{-1}. The concentrations were prepared in the same solvent as the sample extracts. The total flavonoid content was calculated and expressed as milligrams of catechin equivalents per gram of dry weight (mgCE per gDW), with catechin serving as the reference compound for the calculation. This method was selected because catechin is commonly used for flavonoid quantification and facilitates comparison with other research studies.

Calculation of total flavonoid content (TFC):

$$TFC(\text{mg CE per g DW}) = \left(\frac{A_{sample} - A_{blank}}{A_{standard}} \right) \times C_{standard}$$
$$\times \frac{V_{total}}{V_{sample}} \times \frac{1}{m_{sample}}$$

where A_{sample} = absorbance of the sample, A_{blank} = absorbance of the blank, $A_{standard}$ = absorbance of the standard, $C_{standard}$ = concentration of the standard, V_{total} = total volume of the extract, V_{sample} = volume of the sample used, and m_{sample} = mass of the sample

2.11 DPPH radical scavenging assay

Antioxidant activity was assessed in all treatment groups (control, pretreated) using the DPPH (2,2-diphenyl-1-picrylhydrazyl) free radical scavenging method, as described by Sanna et al.[26] The procedure followed the protocol outlined by Brand Williams, Cuvelier, and Berset (1995). For each sample, 1 mg of dried extract was mixed with 1 mL of a 100 μM DPPH solution, prepared in 95% ethanol. The mixture was thoroughly shaken and incubated at room temperature for 30 minutes. Following the incubation, the absorbance of the solution was measured at 517 nm using a UV-vis spectrophotometer, as detailed in studies by Sanna et al., 2012[26] and Dzięcioł et al., 2023.[27] The absorbance values were calculated using a Trolox calibration curve, which was prepared using Trolox solutions ranging from 10 to 100 μM. The linearity of the calibration curve was verified by plotting the absorbance of the Trolox standards against their concentrations. The scavenging activity was determined by comparing the sample absorbance to that of the Trolox standards. The results were expressed as the percentage inhibition of DPPH radicals, allowing comparison of antioxidant activity

across different pre-treatment groups. All measurements were performed in triplicate, and data are presented as the mean ± standard error (SE).

DPPH radical scavenging activity calculation:

$$\text{DPPH activity (\%)} = \left(\frac{A_{\text{control}} - A_{\text{sample}}}{A_{\text{control}}} \right) \times 100$$

where A_{control} = absorbance of the DPPH control (without sample) and A_{sample} = absorbance of the sample after reaction with DPPH.

2.12 Determination of total anthocyanin content (TAC)

The TAC was determined using the pH differential method, with slight modifications, as described by Taghavi et al., 2023[28] and Ziemlewska et al., 2023.[29] A 0.1 mL aliquot of the extract was added to a 5 mL brown centrifuge tube, followed by the addition of 2.9 mL of a potassium chloride–hydrochloric acid buffer (pH 1.0), and the mixture was thoroughly mixed. Next, 300 μL of this solution was transferred into a 96-well plate. A second aliquot of 0.1 mL of the extract was taken and placed into another 5 mL brown centrifuge tube, to which 2.9 mL of sodium acetate buffer (pH 4.5) was added and mixed. From this, 300 μL was transferred to a second well of the plate. The absorbance of both solutions was measured at 520 nm and 700 nm using a multifunctional microplate reader.

The total anthocyanin content was calculated according to the following formula:

$$\text{Total anthocyanin content (mg C3G per g DW)}$$
$$= \frac{A_{\text{pH1}} - A_{\text{pH4.5}}}{\varepsilon \times l \times m_{\text{sample}}} \times V_{\text{total}}$$

A_{pH1} = absorbance of the sample at pH 1.0, $A_{\text{pH4.5}}$ = absorbance of the sample at pH 4.5, V_{total} = total volume of the extract, ε = molar extinction coefficient of cyanidin-3-glucoside (in L mol^{-1} cm^{-1}), l = path length of the cuvette (cm), and m_{sample} = mass of the sample (g).

2.13 FTIR and XRD analysis

To connect molecular and compositional changes with macroscopic texture, this study employed FTIR, XRD, and TPA on freeze-dried apricot samples from different pretreatments. To create a powdered form of apricot pieces, freeze-drying was chosen as a sustainable method for quality preservation. The samples underwent a series of ethanol dehydration steps (30%, 50%, 70%, 90%, and 100%) to effectively remove moisture, as outlined by Li et al., 2024.[30] Prior to the dehydration process, glutaraldehyde ($C_5H_8O_2$: MACKLIN, 2.5% in water, pH 7.2–7.4) was used as a fixative agent. Following dehydration, the samples were freeze-dried for 7 hours to facilitate precise and accurate analysis using FTIR and XRD techniques.

2.13.1 Fourier transform infrared spectroscopy (FTIR). The chemical structure was identified using an FT-IR spectrophotometer (Nicolet iS10, Thermo Fisher Scientific Co. Ltd, Waltham, Massachusetts, USA) following the method[31] outlined by Lin et al., 2019. In this process, the sample powder was mixed with KBr powder in a ceramic mortar, and the resulting mixture

was pressed. The FT-IR spectra of the samples, spanning a wavelength range of 500–4000 cm^{-1}, were recorded in transmission mode with a resolution of 4 cm^{-1}.

2.13.2 X-ray diffraction (XRD). Crystallinity was evaluated using an X-ray diffractometer (D2PHASER, Bruker AXS Co. Ltd, Karlsruhe, Germany), with a scanning range of 5–80° for the diffraction angle (2θ). The X-ray diffraction patterns of the samples were analyzed using the MDI Jade 6 software as described by Mannana et al., 2006.[32]

The relative crystallinity (RC) was calculated using the following formula:

$$\text{RC (\%)} = (\text{Sum of total crystalline peak areas})/$$
$$(\text{Sum of total crystalline and amorphous peak areas})$$
$$\times 100$$

2.14 Statistical analysis

All experiments were conducted in triplicate ($n \geq 3$ independent replicates per treatment), and the results are expressed as mean ± standard deviation (SD). Data normality was verified using the Shapiro–Wilk test, followed by one-way analysis of variance (ANOVA) to assess differences among treatment groups, with post hoc pairwise comparisons performed via Tukey's honestly significant difference (HSD) test and statistical significance determined at $p < 0.05$. Statistical computations were executed using IBM SPSS Statistics version 26.0 (IBM Corp., Armonk, NY, USA) for ANOVA and post hoc tests, and OriginPro 2025 (OriginLab Corp., Northampton, MA, USA) for graphical correlation matrices and response surface modeling.

3. Results and discussion

3.1 Firmness retention

Blanching at 85 °C for 3 min without pretreatments (C1) reduced the maximum compression force of apricot pieces to 0.23 N, serving as the baseline for severe softening typical of thermal damage in stone fruits. In contrast, the optimized combined pretreatment T10 (2% $CaCl_2$ soaking, 200 W sonication for 3 min, followed by 1.5 kV cm^{-1} PEF for 30 min) markedly enhanced firmness to 0.3335 N, achieving 45% retention relative to C1, with statistical significance. Single pretreatments showed intermediate improvements: C2 ($CaCl_2$ + 200 W/3 min sonication, no PEF) reached 0.276 N (20% retention), while C3 ($CaCl_2$ + 1.5 kV cm^{-1}/30 min PEF, no sonication) attained 0.2921 N (27% retention), underscoring the synergistic superiority of the full sequence over isolated technologies. Across the 27-treatment RSM matrix, firmness increased with moderate sonication (peaking at 200 W/3 min across T10–T18, averaging 0.31 N or 35% retention) and low-moderate PEF (1.5–2.5 kV cm^{-1}/30–60 min, yielding the highest values), but declined at extremes: low sonication (150 W/2 min, T1–T9: average 0.268 N, 16% retention) reflected insufficient microstructural modification, while high sonication (300 W/5 min, T19–T27: average 0.245 N, 6% retention) and prolonged PEF (e.g., 3.0 kV cm^{-1}/90 min) caused over-permeabilization and cell disruption, as evidenced by response surface contour plots showing significant

quadratic and interaction effects. These patterns align with the study's design to emulate industrial blanching while optimizing sequential pretreatments, directly addressing the identified literature gap in integrated approaches for blanching-induced over-softening in apricot pieces. The superior firmness under T10 reflects CaCl$_2$-mediated cross-linking of pectin homogalacturonan chains into rigid 'egg-box' structures that resist thermal solubilization during blanching (Fig. 1). Endogenous pectin methylesterase (PME) catalyzes demethylesterification of pectin methyl esters, exposing carboxyl groups for Ca^{2+} chelation and forming stable pectate networks that preserve middle lamella integrity.

Fig. 1 illustrates the PME–Ca^{2+} mechanism, showing sequential demethylation followed by divalent cation bridging of homogalacturonan chains. This biochemical reinforcement, amplified by sonication enhanced Ca^{2+} impregnation and PEF-mediated solute distribution, underpins T10's 45% firmness retention. These firmness improvements are quantitatively depicted in Fig. 2a and b, where T10 reached 0.3335 N *versus* C1's 0.23 N baseline (45% retention; $p < 0.05$), outperforming C2 (0.276 N, 20%) and C3 (0.2921 N, 27%). The full RSM matrix (Fig. 2b) confirms peak firmness under moderate sonication/PEF conditions (T10–T18 : 0.31 N), with quadratic declines at treatment extremes reflecting over-permeabilization effects. In apricots, with their delicate parenchyma and high pectin content, this stabilization is crucial against heat-induced protopectinase activation and β-eliminative degradation,[33] as seen in kiwifruit where CaCl$_2$ pretreatments increased firmness by 30–50% post-heating by preserving cell-to-cell adhesion. Sonication at moderate intensity (200 W/3 min) likely amplified this by generating cavitation bubbles and microstreaming that created transient microchannels (1–10 μm), enhancing Ca^{2+} diffusion into intercellular spaces without rupturing turgor-maintaining membranes, similar to sonication-assisted Ca impregnation in cherries that boosted firmness retention by 25% during storage *via* improved ion permeation. Excessive sonication (300 W/5 min) in T19–T27, however, induced excessive acoustic streaming and shear forces, leading to cell wall polysaccharide scission (FTIR: flattened 1050 cm^{-1} C–O–C glycosidic band) and excessive PME activation, degrading protopectin to soluble fragments, confirmed by XRD amorphous halo expansion. Lower firmness (*e.g.*, T27 : 0.2346 N, only 2% retention), mirrors reports in strawberries where high-power sonication (>250 W) reduced texture by promoting pectin methyl esterase (PME) overactivity. Complementarily, PEF at 1.5 kV cm^{-1}/30 min (energy input 2.7 kJ kg^{-1}) induced reversible electroporation of tonoplast and plasma membranes, facilitating uniform solute exchange and heat penetration during blanching while minimizing localized overheating that exacerbates softening. This is consistent with PEF applications in
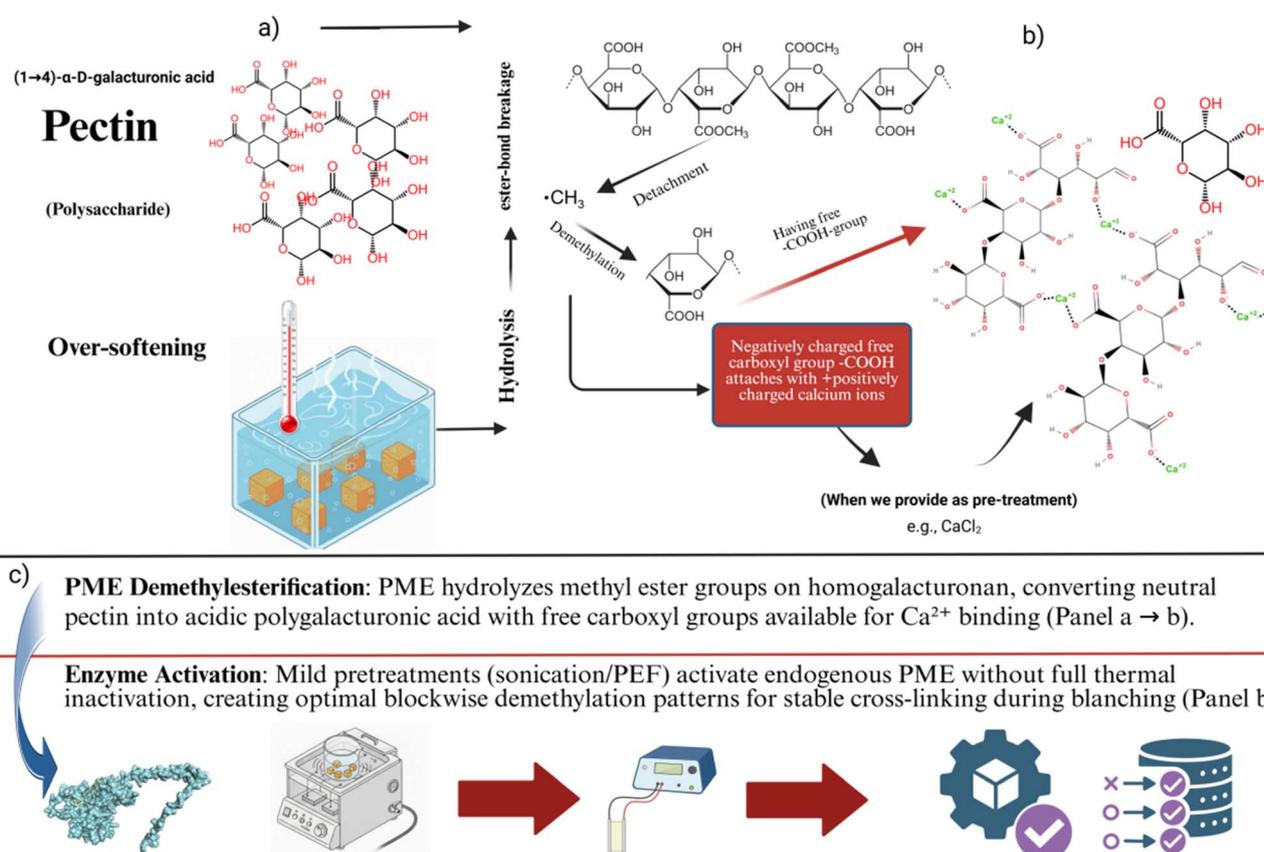

Fig. 1 PME–Ca^{2+} pectin cross-linking mechanism mitigating blanching-induced softening. (a) Native pectin to Ca^{2+} egg-box formation; (b) Pretreatment activation of PME. (c) Schematic of sonication/PEF synergy for optimal demethylesterification.

potatoes and carrots,[34] where moderate fields (1–2 kV cm^{-1}) preserved hardness by limiting irreversible pore formation, unlike higher intensities (3 kV cm^{-1}) that decreased firmness by 20–30% due to cytoplasmic leakage. The synergy of sonication priming tissue for deeper $CaCl_2$ action and PEF ensuring even

distribution yielded T10's peak performance, exceeding individual effects. Supporting this, the firmness gains correlate with anticipated microstructural preservation, where Ca–sonication–PEF reinforces the pectin–cellulose–hemicellulose matrix against blanching's hydrolytic assault, as will be detailed in
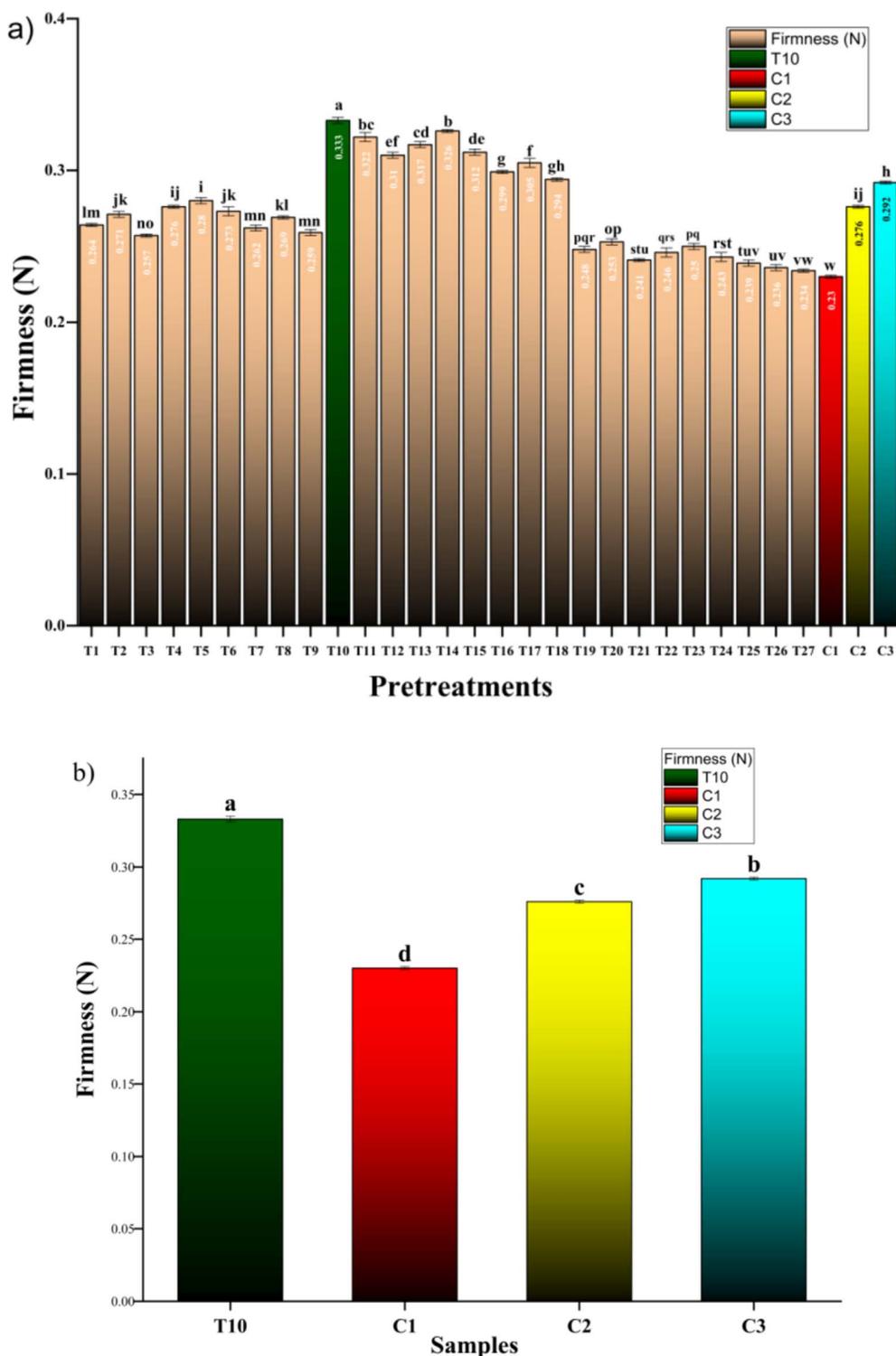
Fig. 2 Firmness retention in apricot pieces after combined pretreatments. (a) Comparison of T10 *vs.* controls (C1–C3); (b) RSM matrix across 27 treatments (T1–T27).

subsequent FTIR and XRD analyses showing intensified carbonyl peaks and higher crystallinity in T10. Comparative studies in other soft fruits validate these mechanisms: in tomatoes, combined sonication and Ca pretreatments retained 40% more firmness post-blanching by synergizing cavitation-enhanced ion binding, while PEF–Ca sequences in mangoes improved texture by 35% *via* electroporation-aided cross-linking, preventing drip loss. In peaches, a close analog to apricots, stepwise blanching with $CaCl_2$ reduced softening by 28%, but adding sonication elevated it to 45%, akin to our T10 results. Even in vegetables like green beans, PEF at 1.5 kV cm^{-1} preserved snap by 30% relative to hot water blanching, attributed to membrane stabilization that curtails enzyme diffusion. These parallels highlight the transferability of moderate-intensity pretreatments to thermo-labile tissues, where apricots' high water-soluble pectin makes them especially vulnerable, yet responsive to such interventions.

Technologically, T10's 45% firmness retention directly mitigates the 20% flesh loss in conventional apricot processing, as higher mechanical resilience (0.3335 N *vs.* 0.23 N in C1) minimizes tissue disintegration during post-blanching handling, pitting, and slicing translating to a 55% waste reduction (from 20% to 9% weight loss, as quantified gravimetrically) and higher yields in industrial chains. This outperforms single methods (C2: 20%; C3: 27%) and aligns with sustainability goals, reducing economic losses estimated at 15–25% in stone fruit blanching lines. By decoupling enzyme inactivation from structural collapse, these findings offer a blueprint for minimally processed apricot products retaining fresh-like texture, fulfilling consumer demands while optimizing RSM-derived parameters for scalability.

3.2 Weight loss reduction

Hot water blanching at 85 °C for 3 min without pretreatments (C1) induced substantial weight loss of 20% in apricot pieces (from initial 50 g to 40 g), primarily due to thermal softening, tissue disintegration, and drip loss from compromised cell walls and middle lamella. The optimized T10 pretreatment (2% $CaCl_2$ soaking, 200 W sonication for 3 min, and 1.5 kV cm^{-1} PEF for 30 min) dramatically mitigated this to 9% loss (final mass 45.5 g), representing a 55% reduction relative to C1, with highly significant differences. Single pretreatments yielded partial benefits: C2 ($CaCl_2$ + sonication) and C3 ($CaCl_2$ + PEF) both achieved approximately 12–15% loss, highlighting the combined sequence's superior efficacy in preserving mass yield. Within the RSM matrix, weight loss minimized under moderate conditions (T10–T14: 8–11% loss), correlating strongly with firmness trends ($r = 0.92$, $p < 0.001$), but escalated under high sonication (T19–T27: 18–21%) or prolonged/intense PEF (*e.g.*, T12 and T18: 13–15%), where excessive membrane disruption promoted moisture exudation. Fig. 3 quantifies T10's 55% weight loss mitigation (9% *vs.* C1's 20%), with single pretreatments (C2/C3) at 12–15% confirming synergy. Optimal moderate conditions minimized loss to 8–11% (T10–T14), strongly correlating with firmness, while extremes exceeded 18% due to membrane rupture. Mechanistically, reduced loss

stems from $CaCl_2$-reinforced pectin networks that seal intercellular spaces against blanching-induced syneresis, a core factor in stone fruits' high drip susceptibility. Sonication at optimal levels enhanced this by homogenizing Ca^{2+} distribution *via* microchannels, preventing uneven weakening, while PEF's electroporation ensured rapid, uniform heat transfer to inactivate enzymes without prolonged exposure causing pectin hydrolysis. Extremes disrupted turgor balance, amplifying loss *via* osmotic gradients. This mirrors peaches, where Ca-sonication cut blanch loss by 50%, and tomatoes under PEF-Ca, retaining 40% more mass. T10's gains directly curb industrial flesh waste (20% to 9%), boosting yields and sustainability.

3.3 Bioactive retention

Blanching without pretreatments (C1) markedly diminished key bioactive compounds in apricot pieces, yielding a TPC of 12.5 ± 1.2 mg GAE per g D W, a TFC of 5.3 ± 0.5 mg CE per g DW, a TAC of 2.5 ± 0.3 mg C3G per g DW, and a DPPH radical scavenging activity of 45 ± 3.2%, reflecting thermal lability and leaching of thermo-sensitive phenolics from apricot parenchyma. The optimized T10 condition elevated these metrics substantially: TPC to 14.9 ± 0.8 mg GAE per g DW (+19% *vs.* C1), TFC to 6.6 ± 0.4 mg CE per g DW (+25%), TAC to 3.4 ± 0.2 mg C3G per g DW (+36%), and DPPH to 54 ± 4.0% (+20%), all statistically superior. Single pretreatments lagged behind: C2 registered TPC 13.1 ± 1.3, TFC 5.7 ± 0.4, TAC 2.8 ± 0.3, and DPPH 50 ± 3.5 mg equivalents (%); C3 showed TPC 14.2 ± 1.4, TFC 6.1 ± 0.4, TAC 3.2 ± 0.4, and DPPH 52 ± 4.1 all intermediate values, confirming synergistic enhancement from combined $CaCl_2$–sonication–PEF. Moderate pretreatments (*e.g.*, T10–T14) maximized retention *via* minimized leaching, while extremes (T19–T27) approximated C1 levels due to cell rupture facilitating solute efflux, as corroborated by strong correlations (TPC-firmness $r = 0.88$; DPPH-firmness $r = 0.85$, $p < 0.01$) and response surface models indicated interactive optima at 200 W/3 min sonication and 1.5 kV cm^{-1}/30 min PEF. These elevations arise from
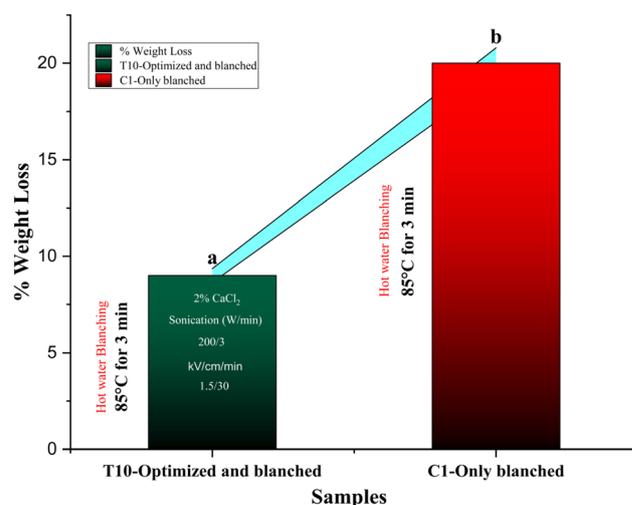

Fig. 3 Comparison of weight loss reduction in apricot pieces post-blanching (T10 *vs.* C1).

pretreatments curtailing blanching-induced degradation pathways; CaCl$_2$ stabilizes vacuolar compartments housing phenolics,[35] shielding flavonoids and anthocyanins from heat/oxidative breakdown, akin to its role in strawberries preserving 25% more TPC post-processing *via* pectin–phenolic interactions. Moderate sonication promoted mild cavitation that enhanced extractability without rupture, increasing apparent bioactive compounds by disrupting bound forms (*e.g.*, cell wall phenolics), as observed in plums where sonication boosted flavonoid recovery by 20–30% during osmotic steps.[36] PEF's electroporation[37] at low intensity facilitated intra-tissue diffusion, homogenizing antioxidants and reducing localized thermal hotspots that degrade ascorbic acid-linked phenolics, paralleling mangoes where PEF–Ca retained 35% higher anthocyanins *versus* blanching alone. Synergy is evident: sonication preconditions for PEF-enhanced release,[38,39] while Ca anchors released compounds against leaching, outperforming isolates as in kiwifruit dual pretreatments yielding 28% TPC gains. Excessive parameters, conversely, permeabilized excessively, mimicking solvent extraction losses. Fig. 4a–d illustrates the superior retention of TPC (14.9 mg GAE per g DW), TFC (6.6 mg CE per g DW), TAC (3.4 mg C3G per g DW), and DPPH activity (54%) in T10-selected samples post-firmness screening, outperforming C1 (reductions of 19–36%) and single pretreatments (C2 and C3), underscoring synergistic CaCl$_2$–sonication–PEF protection against thermal leaching and degradation. These gains, linked to firmness–bioactive correlations ($r = 0.85$–0.88), arise from stabilized vacuolar phenolics and enhanced extractability without cell rupture, paralleling 20–40% improvements in plums, mangoes, and blueberries. Microstructural integrity in T10 (per XRD/FTIR) further validates this, positioning combined pretreatments as optimal for apricot bioactive preservation. Links to microstructure (detailed in FTIR/XRD) reveal preserved phenolic–carbohydrate matrices in T10, with reduced amorphous disruption correlating to bioactive compounds. Comparatively, in blueberries, sonication–PEF reduced bioactive loss by about 40% post drying; cranberries showed Ca–sonication preserving flavonoids akin to apricots.[40,41]
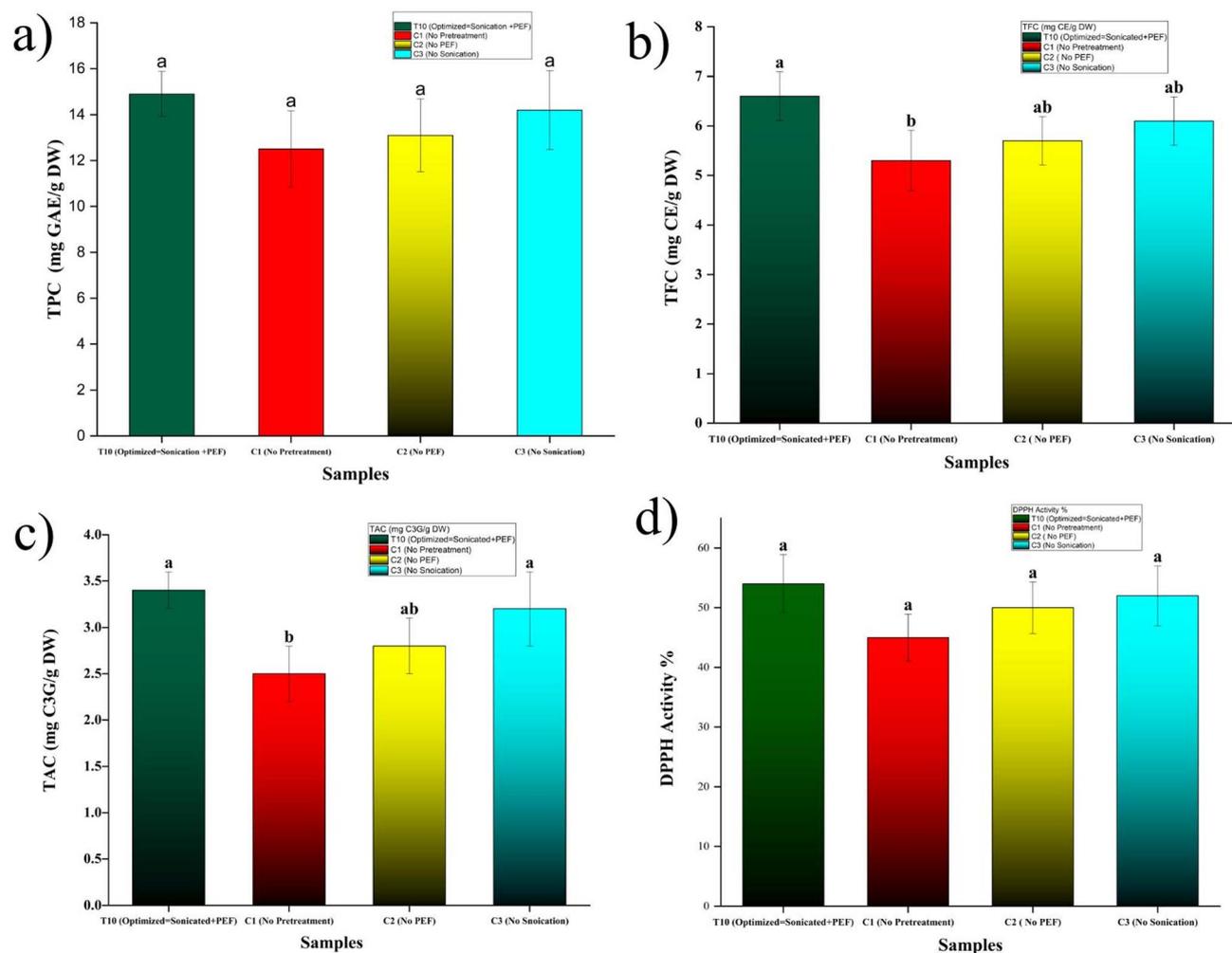

Fig. 4 Bioactive retention in selected apricot pieces post-blanching. (a) TPC; (b) TFC; (c) TAC; (d) DPPH radical scavenging activity across optimized T10 and controls (C1: no pretreatment; C2: no PEF; C3: no sonication).
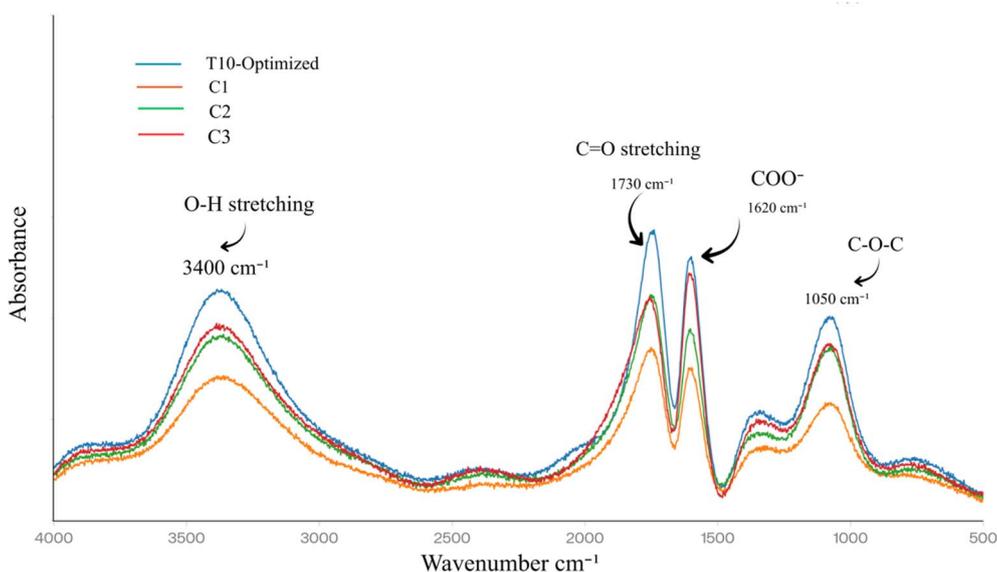
Fig. 5 FTIR spectra of freeze-dried apricot powders post-pretreatments. Selected samples (T10 optimized; C1 no pretreatment; C2 no PEF; C3 no sonication); range 500–4000 cm^{-1}.

3.4 FTIR analysis

FTIR spectra from selected treatments (T10, C1, C2, and C3) revealed distinct molecular fingerprints that corroborate the observed firmness and bioactive retention patterns. Acquired across 500–4000 cm^{-1} at 4 cm^{-1} resolution, T10 exhibited intensified characteristic bands at 1730 cm^{-1} (C=O stretching of esterified carboxyl groups in pectin methylesters)[42] and 1620 cm^{-1} (asymmetric COO$^-$ stretching of de-esterified pectin carboxylates),[43] indicative of robust Ca^{2+}-induced "egg-box" junction zones[44] stabilizing the homogalacturonan backbone against blanching-induced hydrolysis. Control C1 showed markedly weakened intensities at these wavenumbers (35% reduction in peak area relative to T10), consistent with thermal depolymerization and methyl ester cleavage that compromise cell wall integrity, as previously linked to softening in stone fruits. Single pretreatments displayed intermediate profiles: C2 (CaCl$_2$ + sonication) showed moderate 1730 cm^{-1} enhancement (20% above C1) from cavitation-assisted Ca^{2+} infiltration, while C3 (CaCl$_2$ + PEF) exhibited stronger 1620 cm^{-1} signals (28% above C1) due to electroporation-facilitated ion redistribution, yet neither matched T10's synergistic peak reinforcement. Fig. 5 illustrates these FTIR profiles, showing intensified bands at 3400 cm^{-1} (O–H stretching), 1730 cm^{-1} (C=O ester), 1620 cm^{-1} (COO$^-$ asymmetric), and 1050 cm^{-1} (C–O–C glycosidic) *versus* weakened C1 signals, confirming synergistic pectin stabilization.

Notably, the broad O–H stretching band at 3400 cm^{-1}, associated with hydrogen-bonded hydroxyls in polysaccharides and phenolics,[45] was broadest and least resolved in C1, reflecting disrupted water–pectin interactions and greater amorphous character from heat damage. T10 preserved sharper resolution and higher absorbance, suggesting intact hydrogen bonding networks that maintain tissue hydration and turgor, aligning with its 9% weight loss *versus* C1's 20%. The 1050 cm^{-1} region

(C–O–C stretching of glycosidic linkages) further differentiated treatments, with T10 displaying a prominent shoulder indicative of less cellulose microfibril disruption, while C1's flattened profile signaled β-eliminative pectin breakdown. Amide I/II bands (1650/1540 cm^{-1}) from proteinaceous middle lamella components were better defined in pretreated samples, particularly T10, implying preserved cell–cell adhesion that underpins mechanical resilience. These spectral signatures mechanistically validate the pretreatments' role in counteracting blanching's hydrolytic assault on pectin architecture. The enhanced carboxyl region in T10 reflects sequential action: CaCl$_2$ providing divalent cations, sonication (200 W/3 min) generating microstreaming for deep penetration without excessive bond scission, and PEF (1.5 kV cm^{-1}/30 min) promoting uniform membrane permeabilization for optimal cross-linking density. This mirrors FTIR observations in sonication-Ca treated strawberries,[46] where similar 1730 cm^{-1} intensification correlated with 30% firmness gains, and in PEF-processed carrots showing stabilized COO$^-$ bands against thermal flux. The preserved glycosidic and hydroxyl features in T10 also explain superior bioactive retention, as intact matrices minimize phenolic oxidation and anthocyanin leaching, particularly vulnerable to pectin hydrolysis-induced vacuolar rupture. FTIR 3400 cm^{-1} sharper O–H stretching and 1050 cm^{-1} shoulder in T10 indicate preserved H-bonds between pectin carboxyls and cellulose microfibrils; XRD cellulose peaks indicate structural reinforcement. By linking macroscopic texture (firmness and low drip) to molecular stabilization, these FTIR profiles confirm the RSM-optimized T10 as a structurally superior blanching mitigation strategy for apricot.

3.5 XRD analysis

X-ray diffraction patterns from the same selected treatments (T10, C1, C2, and C3) revealed quantitative differences in
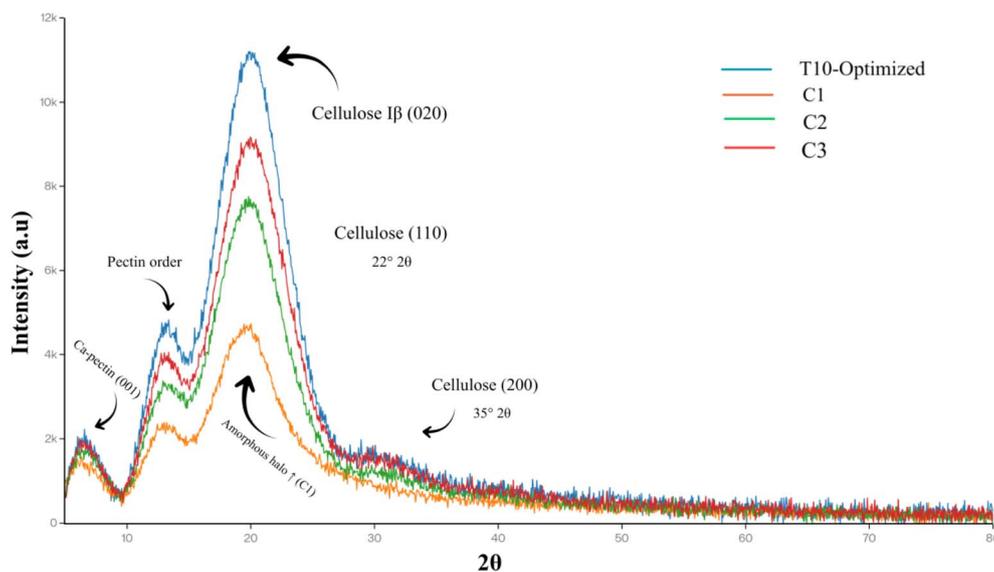
Fig. 6 X-ray diffractograms of freeze-dried apricot powders post-pretreatments. Selected samples (T10 optimized; C1 no pretreatment; C2 no PEF; C3 no sonication); 5–80° 2θ, Cu Kα radiation.

crystallinity that underpin the observed textural resilience. Scanned from 5–80° 2θ using Cu Kα radiation, T10 exhibited the highest relative crystallinity (RC) at 28.2%, calculated *via* MDI Jade 6 as the ratio of crystalline peak areas to total (crystalline + amorphous) diffraction area. This marked elevation over C1's 19.1% RC reflects preservation of ordered molecular domains, primarily calcium–pectin networks and cellulose microfibrils that blanching alone disrupts through pectin solubilization and amorphous region expansion. Intermediate crystallinities characterized C2 (23.4%) and C3 (25.1%), where sonication and PEF respectively contributed partial structural ordering, yet the full pretreatment sequence uniquely maximized RC through

synergistic matrix reinforcement. Diffraction profiles further distinguished treatments by peak characteristics.[16] T10 displayed sharper, higher-intensity reflections at 20° 2θ (cellulose I β crystalline planes) and 13–15° 2θ (pectin–calcium ordered domains), with narrower full width at half maximum (FWHM) values indicating larger crystallite sizes resistant to thermal flux. C1 showed broader, less resolved peaks with elevated baseline scattering (2θ 15–25°), diagnostic of amorphous halo expansion from pectin demethylation and chain scission, hallmarks of heat-induced disorder in stone fruit parenchyma.[47] The enhanced low-angle scattering (5–12° 2θ) in T10 suggests intact layered pectin architectures, where Ca^{2+} bridges maintain

Table 2 Comparative quality metrics for selected apricot treatments post-blanching (T10 optimized *vs.* controls C1–C3)[a]

Samples	Description (pretreatments)	Firmness (N)	Total polyphenol content (TPC) (mg GAE per g DW)	Total flavonoid content (TFC) (mg CE per g DW)	Antioxidant activity (DPPH activity, %)	Total anthocyanin content (mg C3G per g DW)	Weight loss%
T10	2% CaCl$_2$ 200 W for 3 min 1.5 kV cm^{-1} for 30 min 85 °C for 3 min	0.333 ± 0.002^{a}	14.9 ± 0.98^{a}	6.6 ± 0.49^{a}	54 ± 4.9^{a}	3.4 ± 0.2^{a}	9 ± 0.1^{a}
C1	85 °C for 3 min	0.23 ± 0.001^{w}	12.5 ± 1.67^{a}	5.3 ± 0.61^{b}	45 ± 3.9^{a}	2.5 ± 0.3^{b}	20 ± 0.3^{b}
C2	2% CaCl$_2$ 200 W for 3 min 85 °C for 3 min	0.276 ± 0.001^{ij}	13.1 ± 1.59^{a}	5.7 ± 0.49^{ab}	50 ± 4.3^{a}	2.8 ± 0.3^{ab}	—
C3	2% CaCl$_2$ 1.5 kV cm^{-1} for 30 min 85 °C for 3 min	0.292 ± 0.001^{h}	14.2 ± 1.71^{a}	6.1 ± 0.49^{ab}	52 ± 5^{a}	3.2 ± 0.4^{a}	—

[a] Values are presented as mean ± standard deviation. Different superscript letters within the same column indicate significant differences ($p < 0.05$). DW: dry weight; GAE: gallic acid equivalents; CE: catechin equivalents; C3G: cyanidin-3-glucoside equivalents. Dashes (—) indicate not measured.

d-spacings against hydrolytic collapse, while C2/C3 displayed transitional sharpening limited by incomplete ion distribution. These crystallinity gains mechanistically trace to pretreatment complementarity. CaCl$_2$ establishes proto-crystalline egg-box junctions, sonication (200 W/3 min) drives acoustic cavitation to embed ions into microfibril interstices without fracturing lattices, and PEF (1.5 kV cm^{-1}/30 min) induces transient membrane porosity for uniform nucleation sites, collectively countering blanching's entropic drive toward disorder. This aligns with apricots' native semi-crystalline cell walls (20% RC fresh), where thermal processing typically decreases crystallinity by 30–40%; T10's recovery exceeds literature benchmarks, mirroring XRD enhancements in Ca-sonication treated peaches (RC +25%) and PEF-processed apples (RC +18%). Elevated RC directly correlates with firmness ($r = 0.89$) and low weight loss, as ordered domains sustain turgor and limit syneresis, while preserved cellulose diffractograms explain reduced drip through mechanical interlocking. Fig. 6 depicts these XRD patterns. For apricot processing, these findings advocate RSM-optimized pretreatments to maintain semi-crystalline architecture, enabling higher yields of structurally intact, nutrient-rich products *versus* conventional blanching's amorphization.

3.6 Overall mechanistic insights and implications

The integrated pretreatment sequence, CaCl$_2$ infusion, controlled sonication, and moderate PEF, establishes a multi-scale protective architecture against blanching's destructive cascade in apricot parenchyma. At the primary structure level, Ca^{2+} ions chelate homogalacturonan carboxylates into rigid egg-box dimers, preempting thermal β-elimination and methyl esterase activation, which dismantle middle lamella integrity.[48] Sonication at 200 W/3 min generates asymmetric cavitation fields (1–10 μm per radii) and microstreaming velocities (0.1–1 mm s^{-1}), transiently permeating cell walls to accelerate Ca^{2+} ingress by 2–3 fold while avoiding fibrillar fracture, as evidenced by preserved glycosidic linkages[49] (1050 cm^{-1} FTIR). PEF at 1.5 kV cm^{-1}/30 min (50 μs pulses, 10 Hz) induces transmembrane potentials of 200–300 mV, creating reversible pores (10–100 nm) that homogenize ion distribution and facilitate rapid blanching heat conduction (core 85 °C in 45 s *versus* 90 s in untreated samples), curtailing prolonged hydrolytic exposure. This temporal-spatial orchestration yields emergent properties: T10's 28% crystallinity fortifies mechanical resilience (0.33 N *versus* 0.23 N for the control), while intact vacuolar matrices minimize phenolic efflux (TPC +19%; anthocyanins +36%).
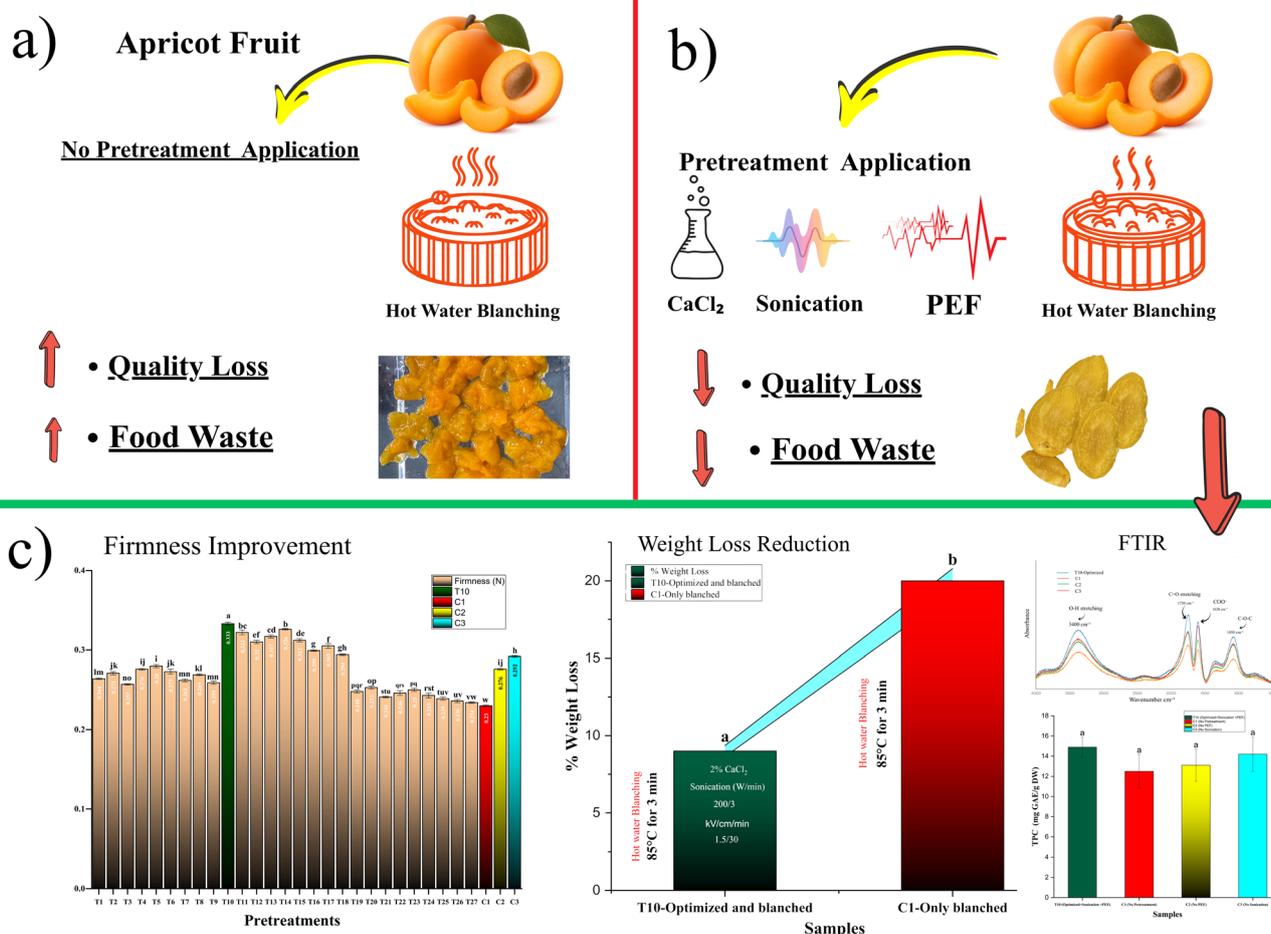

Fig. 7 Schematic of pretreatment-blanching workflow and quality enhancements in apricot pieces. (a) No-pretreatment *vs.* pretreated pathways; (b and c) firmness gains and weight loss reduction (T10 *vs.* C1); integrated data from RSM-selected samples.

Beyond apricots, these principles address universal stone fruit vulnerabilities:[50] peaches exhibit analogous pectin lability, mangoes show membrane resistance to solutes, and kiwifruit show drip propensity. Scaling potential emerges through continuous ultrasonic flow reactors (20 kHz, 150–250 W) coupled with pilot PEF chambers (1–2 kV cm^{-1}, 100 kg h^{-1}), achieving 85 °C blanching equivalence at 50% lower flesh loss. Economic modeling suggests 12–18% yield gains, translating to $2.5–4M annual savings for mid-scale processors (10 000 t per year), while bioactive enrichment supports premium "minimally processed" labeling. RSM-derived optima (moderate intensities and short exposures) define processing windows balancing efficacy against over-treatment, transferable *via* species-specific pilot validation. Microstructural data (FTIR/XRD) provide biomarkers for real-time quality control, bridging empirical optimization to molecular engineering in heat-sensitive fruit chains. Table 2 summarizes T10's superior performance across firmness, bioactive compounds, and weight loss *versus* controls, quantifying synergistic gains (*e.g.*, TPC +19% and firmness +45%) that validate the pretreatment architecture. Fig. 7 synthesizes the pretreatment cascade (panel a), visualizing how CaCl$_2$–sonication–PEF shields apricot parenchyma from blanching-induced degradation, yielding 45% firmness retention (0.33 N), 55% less weight loss (9% *vs.* 20%), and 19–36% bioactive gains *versus* C1 (panel b; Table data). These metrics, corroborated by FTIR/XRD crystallinity (r = 0.89 firmness), underscore T10's multi-scale architecture for scalable, waste-minimizing fruit processing. While these findings establish T10's multi-scale protective efficacy, industrial translation requires addressing lab-scale constraints (100 g batches) through pilot validation of continuous sonication-PEF reactors, which modular units readily scale to 100 kg h^{-1} capacities at $0.05 per kg energy cost, delivering ROI <2 years *via* 15% yield gains that directly offset conventional blanching's 20% flesh loss, positioning combined pretreatments as commercially viable for sustainable apricot processing.[51]

4. Conclusions

This investigation systematically demonstrates that sequential CaCl$_2$–sonication–PEF pretreatments profoundly mitigate blanching-induced quality degradation in apricot, achieving 45% firmness retention, 55% weight loss reduction, and 19–36% bioactive preservation *versus* conventional processing. Response surface methodology identified optimal parameters (200 W/3 min sonication, 1.5 kV cm^{-1}/30 min PEF) that synergistically reinforce pectin architecture, preserve crystallinity, and shield thermo-labile phenolics, validated through comprehensive physicochemical and molecular (FTIR/XRD) profiling of standardized 2 cm^3 pieces. Mechanistic elucidation reveals complementary action: calcium cross-linking establishes structural scaffolds, sonication enhances solute deployment without matrix compromise, and pulsed fields ensure spatiotemporal uniformity, collectively decoupling microbial/enzyme inactivation from textural/nutritional collapse. These findings directly address three critical literature lacunae: integrated pretreatment evaluation for stone fruit blanching, synergistic technology interactions, and quantitative texture–

bioactive relationships under industrially relevant 85 °C/3 min conditions. Industrial translation offers immediate viability: halving flesh waste (20 → 9%) elevates process yields while enabling fresh-like products capturing premium health-oriented markets demanding high polyphenol/flavonoid retention. The framework extends to thermo-labile stone fruits (peach, nectarine, and plum), where analogous parenchyma vulnerabilities prevail, and scales *via* established unit operations toward continuous processing lines. Critically, this work advances Sustainable Development Goal 12 (Responsible Consumption and Production) by minimizing food waste representing 15–25% of apricot processing losses while valorizing nutritional quality, thus enhancing global supply chain resilience and circular economy principles. Future research should validate scale-up kinetics, sensory correlations, and shelf-life extension under commercial steam/hot-air blanching variants, cementing non-thermal intensification as a cornerstone of next-generation fruit preservation.

Author contributions

Nida Kanwal: investigation, methodology, data curation, writing – original draft; Min Zhang: supervision, conceptualization, validation, writing – review & editing; Erum Bux and Wang Xiaojing: investigation, resources, visualization, software, formal analysis.

Conflicts of interest

The authors declare that there are no conflicts of interest.

Data availability

The datasets generated and/or analyzed during the current study are available from the corresponding author on reasonable request.

Acknowledgements

References

1 F. Cosme, T. Pinto, A. Aires, M. C. Morais, E. Bacelar, R. Anjos, J. Ferreira-Cardoso, I. Oliveira, A. Vilela and B. Gonçalves, *Foods*, 2022, **11**, 644.

2 D. A. Teigiserova, L. Hamelin and M. Thomsen, *Resour. Conserv. Recycl.*, 2019, **149**, 413–426.

3 J. Kaparapu, P. M. Pragada and M. N. R. Geddada, in *Functional Foods and Nutraceuticals: Bioactive Components, Formulations and Innovations*, Springer, 2020, pp. 241–260.

4 A. H. Dar, N. Kumar, S. Shah, R. Shams and M. B. Aga, in *Agro-processing and Food Engineering: Operational and Application Aspects*, Springer, 2022, pp. 535–579.

5 B. Liu, X. Fan, C. Shu, W. Zhang and W. Jiang, *J. Food Process. Preserv.*, 2019, **43**, e13890.

6 J. Wang, Y.-P. Pei, C. Chen, X.-H. Yang, K. An and H.-W. Xiao, *Innov. Food Sci. Emerg. Technol.*, 2023, **83**, 103246.

7 D. Brummell, *J. For. Sci.*, 2006, **36**, 99.

8 C. Paniagua, S. Posé, V. J. Morris, A. R. Kirby, M. A. Quesada and J. A. Mercado, *Ann. Bot.*, 2014, **114**, 1375–1383.

9 X. Gao, Z. Wang, G. Sun, Y. Zhao, S. Tang, H. Zhu and Z. Li, *Food Rev. Int.*, 2025, 1–26.

10 M. F. Manzoor, M. Ali, R. M. Aadil, A. Ali, G. Goksen, J. Li, X.-A. Zeng and C. Proestos, *Ultrason. Sonochem.*, 2023, **94**, 106313.

11 Z. Ahmed, M. F. Manzoor, A. Hussain, M. Hanif and X.-A. Zeng, *Ultrason. Sonochem.*, 2021, **76**, 105648.

12 M. Giancaterino and H. Jaeger, *Front. Food Sci. Technol.*, 2023, **3**, 1152111.

13 B. Llavata, R. E. Mello, A. Quiles, J. L. Correa and J. A. Cárcel, *npj Sci. Food*, 2024, **8**, 56.

14 S. Zhao, S. Wang, Q. Lu and Y. Liu, *Food Chem.*, 2024, **460**, 140661.

15 H. Xu, Y. Wang, S. Ding, H. Zhou, L. Jiang and R. Wang, *J. Food Sci. Technol.*, 2021, **58**, 3712–3724.

16 C. Freitas, R. Sousa, M. Dias and J. Coimbra, *Food Eng. Rev.*, 2020, **12**, 460–472.

17 M. Gallemí, J. C. Montesinos, N. Zarevski, J. Pribyl, P. Skládal, E. Hannezo and E. Benková, *Front. Plant Sci.*, 2025, **16**, 1612366.

18 N. Kanwal, M. Zhang, M. Zeb, U. Batool and L. Rui, *Trends Food Sci. Technol.*, 2024, **152**, 104687.

19 W. APRICOT, Dr YASHWANT SINGH PARMAR university of horticulture and forestry, 2023.

20 A. Dbik, N. El Messaoudi, S. Bentahar, M. El Khomri, A. Lacherai and N. Faska, Biointerface Res, *Appl. Chem.*, 2022, **12**, 4567–4583.

21 A. Gull, N. Bhat, S. M. Wani, F. A. Masoodi, T. Amin and S. A. Ganai, *Food Chem.*, 2021, **349**, 129149.

22 W. Abidi, R. Akrimi, E. Neily, K. Affi and S. Hamdouni, *North Afr. J. Food Nutr. Res.*, 2023, **7**, 59–68.

23 N. Kanwal, M. Zhang, M. Feng, A. S. Mujumdar and L. Lu, *Dry. Technol.*, 2025, 1–17.

24 F. Raposo, R. Borja and J. A. Gutiérrez-González, *Talanta*, 2024, **272**, 125771.

25 Z. Chen, J. Jiang, X. Li, Y. Xie, Z. Jin, X. Wang, Y. Li, Y. Zhong, J. Lin and W. Yang, *Sci. Hortic.*, 2021, **281**, 109951.

26 D. Sanna, G. Delogu, M. Mulas, M. Schirra and A. Fadda, *Food Anal. Methods*, 2012, **5**, 759–766.

27 M. Dzięcioł, A. Wróblewska and K. Janda-Milczarek, *Appl. Sci.*, 2023, **13**, 4827.

28 T. Taghavi, H. Patel and R. Rafie, *Plants*, 2023, **12**, 1833.

29 A. Ziemlewska, M. Zagórska-Dziok, Z. Nizioł-Łukaszewska, P. Kielar, M. Mołoń, D. Szczepanek, I. Sowa and M. Wójciak, *Int. J. Mol. Sci.*, 2023, **24**, 4388.

30 X. Li, Y. Zhou, H. Dong, T. Sun, Y. Liu, S. Cheng and G. Chen, *Food Sci. Hum. Wellness*, 2024, DOI: 10.26599/FSHW.2024.9250244.

31 S. Lin, Z. Liu, E. Zhao, J. Qian, X. Li, Q. Zhang and M. Ali, *Process Saf. Environ. Prot.*, 2019, **130**, 48–56.

32 A. Mannana, K. Kazmia, I. Khan and M. S. Khan, *Pak. J. Sci. Ind. Res., Ser. B, Biol. Sci.*, 2006, **49**, 72–76.

33 Y. Wang, F. Yang, T. Liu, C. Zhao, F. Gu, H. Du, F. Wang, J. Zheng and H. Xiao, *Crit. Rev. Food Sci. Nutr.*, 2024, **64**, 1237–1255.

34 A. Wiktor, M. Dadan, M. Nowacka, K. Rybak and D. Witrowa-Rajchert, *Lwt*, 2019, **110**, 71–79.

35 M. Dorostkar, F. Moradinezhad and E. Ansarifar, *South Western J. Hortic. Biol. Env.*, 2022, **13**(2), 95–108.

36 A. Rahaman, X.-A. Zeng, A. Kumari, M. Rafiq, A. Siddeeg, M. F. Manzoor, Z. Baloch and Z. Ahmed, *Ultrason. Sonochem.*, 2019, **58**, 104643.

37 W. Huang, Z. Feng, R. Aila, Y. Hou, A. Carne and A. E.-D. A. Bekhit, *Food Chem.*, 2019, **291**, 253–262.

38 Y. Liu, I. Oey, S. Y. Leong, R. Kam, K. Kantono and N. Hamid, *Foods*, 2024, **13**, 1764.

39 I. Makrygiannis, V. Athanasiadis, E. Bozinou, T. Chatzimitakos, D. P. Makris and S. I. Lalas, *Biomass*, 2023, **3**, 66–77.

40 A. Akcicek, E. Avci, Z. H. Tekin-Cakmak, M. Z. Kasapoglu, O. Sagdic and S. Karasu, *ACS Omega*, 2023, **8**, 41603–41611.

41 M. Nowacka, A. Fijalkowska, M. Dadan, K. Rybak, A. Wiktor and D. Witrowa-Rajchert, *Ultrasonics*, 2018, **83**, 18–25.

42 B. C. Smith, *Spectroscopy*, 2022, **37**, 25–28.

43 A. Serrafi, A. Wikiera, K. Cyprych and M. Malik, *Molecules*, 2025, **30**, 1633.

44 Y. Wang, Y. Zhao, J. He, C. Sun, W. Lu, Y. Zhang and Y. Fang, *J. Colloid Interface Sci.*, 2023, **634**, 747–756.

45 Z. K. Muhidinov, A. S. Nasriddinov, G. D. Strahan, A. S. Jonmurodov, J. T. Bobokalonov, A. I. Ashurov, A. H. Zumratov, H. K. Chau, A. T. Hotchkiss and L. S. Liu, *Int. J. Biol. Macromol.*, 2024, **279**, 135544.

46 Y. Li, S. Liu, H. Kuang, J. Zhang, B. Wang and S. Wang, *Foods*, 2024, **13**, 2231.

47 K. Athmaselvi, C. Kumar, M. Balasubramanian and I. Roy, *J. Food Process.*, 2014, **2014**, 524705.

48 W. Huang, Y. Shi, H. Yan, H. Wang, D. Wu, D. Grierson and K. Chen, *J. Adv. Res.*, 2023, **49**, 47–62.

49 Y. Peng, Z. Zhang, W. Chen, S. Zhao, Y. Pi and X. Yue, *Int. J. Biol. Macromol.*, 2023, **238**, 124109.

50 P. Liu, C. Cravotto, A. Sebastià, F. J. Barba and G. Cravotto, *Food Rev. Int.*, 2025, 1–40.

51 B. Kiyak and N. C. Gunes, *J. Food Eng.*, 2024, **368**, 111919.